Rafidain Journal of Science

https://rsci.uomosul.edu.iq

Vol. 34, No. 3, pp. 91-101, 2025 (September)

Study of the Effect of Using Various Ceramic Powders in Thermal Spraying Technology on the Sliding Corrosion Resistance of Steel Alloys (AISI446)

Ahmed S.A. Hussein **Yahya A.K. Salman** **Edrees E. Khadeer**

Department of Physics/ College of Science/ University of Mosul/ Mosul/ Iraq.

p-ISSN: 1608-9391
e -ISSN: 2664-2786

Article information

Received: 17/1/2025
Revised: 12/4/2025
Accepted: 22/4/2025

DOI: 10.33899/rjs.2025.189221

corresponding author:
Ahmed S.A. Hussein
ahmed.scp99@student.uomosul.edu.iq
Yahya A.K. Salman
Yahya200138@uomosul.edu.iq
Edrees E. Khadeer
dr.adress@uomosul.edu.iq

ABSTRACT

Different phenomena require separate measurement of corrosion rate and sliding wear rate. The chemical decomposition between materials contacting their environments results in corrosion but the friction generated by moving surfaces causes sliding wear. Scientists studied the sliding wear resistance of AISI 446 stainless steel alloy which received thermal coatings made from diverse concentrations of silicon oxide, silicon carbide and nickel-aluminum (SiC + SiO2 + Ni-Al) ceramic powders. Thermal spray welding torch (QH-2/H) served as the equipment to apply the coatings. The testing procedure followed ASTM D5963 standard specifications for a pin-on-dish apparatus which operated at different vertical loads with speeds and dish surface parameters. The experimental analysis revealed that the utilized coatings demonstrated superior sliding wear resistance than the original base alloy after the inclusion. The wear rate of all tested samples rose steadily while the loads increased. The alloy N_1 achieved the lowest corrosion rate while containing 75% silicon carbide combined with 25% Ni-Al binder material. The alloy manifested a -60.36% decline of corrosion rate against the base alloy when subjected to 26N of vertical force. The alloy (N_6) composed of 75% SiC and no SiO_2 generated the minimal sliding wear rate of 180 rev/min because of its -45.42% enhanced performance. Sample (N_1) demonstrated decreased performance compared to the uncoated alloy even though its abrasive surface generated better wear resistance. The result showed an increase of -13.24% in wear rates.

Keywords: Alloys, sliding corrosion resistance, thermal spraying.

INTRODUCTION

Thermal spraying technology is used in many modern industries to apply a coating to surfaces, where molten or semi-molten materials are pushed to enhance the properties of the surface to be treated. This technology includes a variety of materials such as metals, alloys, and ceramics, and is applied to various types of stainless steel, giving them excellent resistance to mechanical and chemical corrosion at temperatures up to, making them suitable for many thermal applications such as steam generators and furnace parts (Mazin *et al*., 2022). Surface studies have received great attention in many industrial applications that change the surface of the manufactured metal or alloy to achieve specific properties. This modification of the surface occurs in various ways, often using heat treatments or chemical heat to achieve precise modifications or diffusion of material molecules such as carbon and nitrogen (Wang and Lee, 1997). It is possible to obtain surface properties different from the uncoated base alloy. Thermal spraying techniques depend on the thermal or kinetic energy of the melted raw material and the method of pushing it into the base alloy as well as in the form of particles or droplets of the spray material. Many materials can be thermally sprayed, according to the compatibility between the specific process and the materials, the mechanical and physical properties of coated materials differ from those of their components when they are uncoated, such as toughness, hardness, friction resistance, fatigue life, corrosion resistance, insulation, and thermal conductivity (Tao *et al*., 2009). Many researchers have focused their efforts on improving the mechanical properties of iron alloys and increasing their ability to resist friction and corrosion. The results showed that the rate of erosion corrosion increases linearly with many variables such as vertical sliding distance, linear velocity, and the nature of the abrasive surface (Askeland *et al*., 2012). The experimental results also showed that the corrosion rate also increases with the increase of other factors such as humidity, heat generated as a result of the friction process, sliding distance, and applied load (Vafaeenezhad *et al*., 2012). Therefore, these studies recommended the need to ensure the selection of appropriate materials and coating methods to enhance corrosion resistance.

MATERIALS AND METHOD

Materials

AISI446 stainless steel alloy was chosen as the base alloy because it is used in the petroleum industry, power generation equipment and chemical processing, due to its excellent properties in resisting corrosion and oxidation at high temperatures, as it can be placed in thermal environments ($1100^{\circ}C$) without losing its mechanical properties in addition to its resistance to corrosion resulting from erosion and crosin. (Table 1) shows the weight percentages of the base alloy (AISI 446).

Table 1: Weight ratios of stainless-steel alloy to base alloy (N_o) (AISI 446) (Tsukizoe and Ohmae, 1983**).**

Alloy designation	The code of Sample	Chemical composition, weight percent							
AISI 446	N_o	Fe	Cr	Mn	Si	Ni	C	P	S
		73	23.0-27.0	1.50	1.0	0.25	0.20	0.040	0.030

Table 2: Weight ratios of bond coating powder (N_1).

Powde name	Chemical equation	Sample Code	Chemical composition, wt%	
Bond coating	Ni-Al	N_1	Ni	Al
			50	50

Table (3) shows the weight percentages of ceramic powders used as thermal barrier coatings.

Table 3: Weight ratios of the bond and thermal barrier coating powder.

Powder name	Chemical Formula	Sample Code	Chemical composition, wt%		
			SiC	SiO_2	Ni-Al
Thermal barrier coating (TBC)	(SiC+SiO_2+Ni-Al)	N_2	15	60	25
		N_3	30	45	25
		N_4	45	30	25
		N_5	60	15	25
		N_6	75	0	25
		N_7	0	75	25

Samples preparation

The sliding wear resistance test samples for AISI446 stainless steel alloy were designed as shown in Fig. (1).

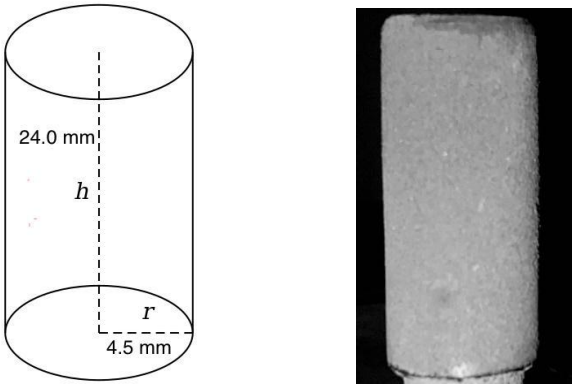

Fig. 1: Corrosion test sample.

This process includes several stages starting with roughening the samples using (320#) sandpaper, then washing them with soap and water, then immersing them in an acetone liquid solution using an ultrasonic cleaning device for (480 sec) to remove any remaining impurities and contaminants, ensuring the cleanliness of the surface. Then they are washed again with distilled water and dried quickly using hot air, then placed in sealed bags where they become ready for the coating process.

Coating processes

The flame spray system was designed and assembled from the local market as shown in Fig. (2). The samples were fixed on an electric motor that rotates at a constant speed to maintain the uniform distribution of the paint on the part to be coated, and it is (12 cm) away from the nozzle of the thermal spray gun. The thermal gun is used to spray the powder placed in the crucible by pressing the regulators fixed in the body of the thermal gun so that a thermal flame is produced from burning acetylene gas and oxygen gas in a stream that includes a mixture of the two gases. This gas stream carries the paint powder stored in the reservoir (tank) at the top of the spray gun to melt and flow smoothly and for the molten paint to adhere well to the surface of the samples. To obtain a constant rate for the mixture of gas and molten powder, the pressure of the oxygen gas should not exceed (4.07 Bar) and the pressure of the acetylene gas should not exceed (0.7 Bar). The spraying process begins by heating the sample for (10 sec) using an oxy-acetylene torch, and for the coating process to be completed on the surface of the sample to be coated, it takes (20 sec), then the samples are left in the air to cool. Fig. (2) shows the spraying system used in the coating process.

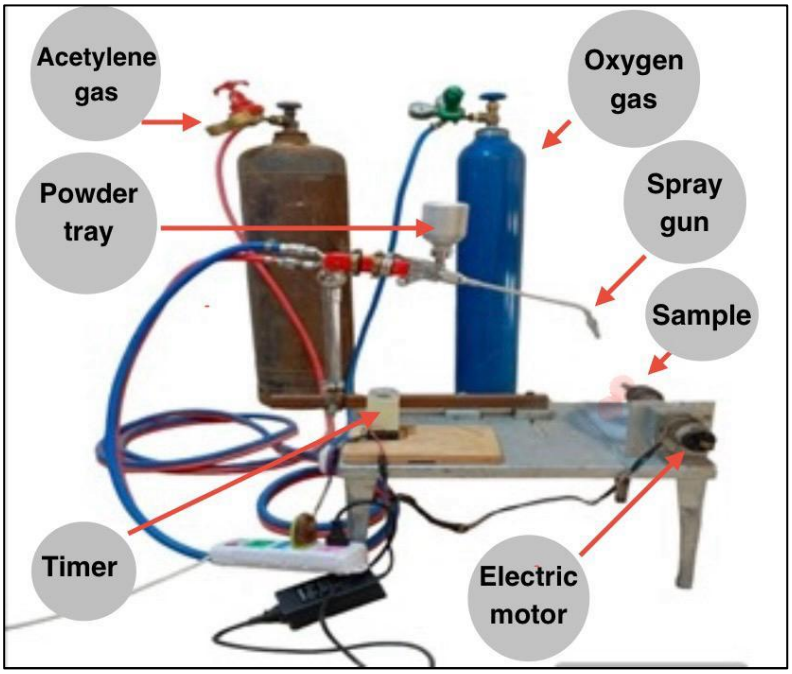

Fig. 2: Thermal spray system.

Thermal spraying

The powder is sprayed with the flame resulting from mixing oxygen with acetylene. The flame can be controlled (increased or decreased) by changing the oxygen ratio, and then the coating process begins, as shown in Fig. 3(b).

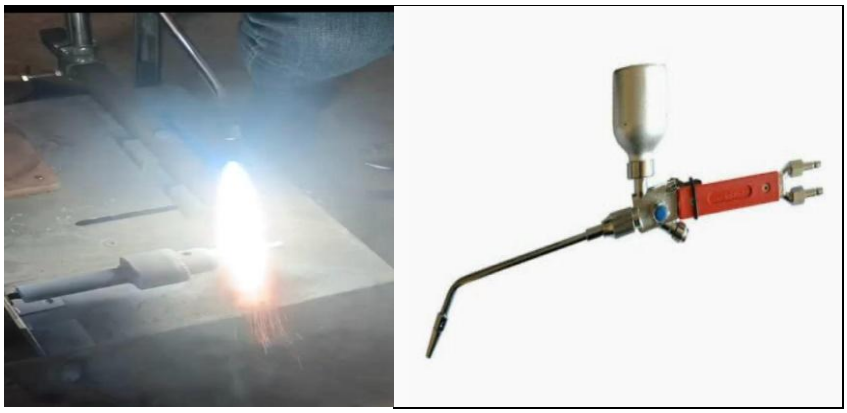

(a) **(b)**

Fig. 3: a) Thermal spray torch. b) Coating procedure.

The coating process was carried out using a Chinese-made flame spray welding torch model (QH-2/H) shown in Fig. 3(a). (Table 4) shows the changes established in the thermal spraying process while maintaining the base alloy temperature within the range (before the spraying process, in order to avoid peeling during the final cooling stage).

Table 4: Thermal spraying process parameters.

Mixing Oxy-Acetylene	4: 0.7 Bar
Flame spray temp	$2500^{\circ}C$
Powder feeding	4.177 gm/min
Spraying distance	12 cm
powder particle size	25-75 μm
Time spent coating	10 to 20 sec

Sliding wear test

The sliding wear test was conducted at room temperature using the gravimetric method on all samples designed for this purpose. This was done to determine the mechanical wear rates in both coated and uncoated samples, as they are affected by changes in applied loads, speed, or the nature of the abrasive surface. Precautions were taken to reduce the testing period for each sample, aiming to minimize the effect of temperature, which is a factor that influences sliding wear rates.

The first part of the test involved using several loads while keeping the rotational speed of the friction disc (V), the radius of the friction circle formed by the sample (r), the roughness of the friction surface, and the sliding duration (t) constant.

The second part focused on changing the linear sliding speed while keeping the applied load fixed.

In the third part, the type of the abrasive surface was changed, while both the applied load and speed remained constant. The table below shows the key variables and constants tested on the samples during the test period.

Table 5: Sliding wear test parameters

Variable friction nature (100, 180, 240, 320, 400) #	Variable sliding velocity (60, 90, 120, 150, 180) min/sec	Variable load (10N, 14N, 18N, 22N, 26N)
r=20 mm, t=300 sec V=120 min/sec, 320# Weight=18N	r=20 mm, t=300 sec 320# Weight=18N	r=20 mm, t=300 sec V=120 min/sec

A sliding wear apparatus designed according to ASTM D5963 specifications, with a screw-on-disc arrangement, was used. The aim of this arrangement is to achieve a direct contact condition between the cylindrical specimen and the rotating disc under the influence of vertical load, which allows the study of wear effects under different conditions, as shown in Fig. (4).

Fig. 4: Corrosion testing device.

The device consists of a variable speed motor. The device also has a steel arm attached at one end to the body of the device. The other end has a holder at its end to fix the sample in its upper part. To place loads on its upper part, this part, fixed at its end, slides on the rotating disc, the wear rate is practically calculated as follows (Bandar *et al.*, 2012):

$$\Delta W = W_1 - W_2 \quad \ldots\ldots\ldots (1)$$

$$Wear\ reat = \frac{\Delta W}{S_D} \left[\frac{gm}{cm}\right] \ldots\ldots\ldots (2)$$

Where:
ΔW: Denotes the variation in mass (gm).
W_1: Sample mass before the test (gm).
W_2: Sample mass after the test (gm).
S_D: The distance of sliding (cm) is articulated by the subsequent equation:

$$S_D = t.v \qquad \ldots\ldots\ldots\ldots (3)$$

Where:
t: The time of sliding (seconds), v: Sliding speed (cm/sec), derived from the following equation:

$$V = \pi DN \quad \ldots\ldots\ldots\ldots\ldots\ldots (4)$$

Where:
N: Disk speed (rpm), D: Sliding diameter (cm).
r: Sliding radius (cm).
By substituting equations (3) and (4) in equation (2), we get:

$$\text{Wear reat } (W.R) = \frac{\Delta W}{(2\pi r.\,t.\,N)/60} \quad \ldots\ldots (5)$$

RESULTS AND DISCUSSION

The curves drawn between the wear rate and the change in the applied loads, shown in Fig. (5), generally show that the wear rate of both the base alloy and the coated one increases with the increase in the applied load. The reason for this is that the increase in the plastic deformation at the tops of the surface protrusions of the samples leads to an increase in the density of dislocations (Eyre, 1976).

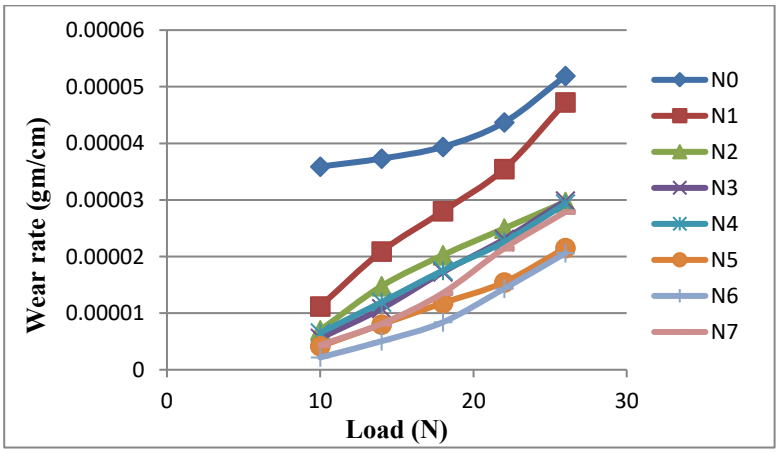

Fig. 5: Sliding wear rate of coated and uncoated samples at different loads.

This leads to an increase in the hardness of the material and it gradually becomes brittle, which causes an increase in the accumulation of dislocations and the formation of small gaps that unite to form small cracks on the surface of the alloy, whether coated or uncoated. The small cracks develop or expand and move under the influence of stresses towards weak areas, which leads to the formation of larger cracks as a result of their rapid accumulation. The convergence of these cracks contributes to the removal of thin layers of the alloy in the direction of the sliding movement, which results in wear debris particles, which are formed as a result of fatigue or exhaustion in the surface layers (Bandar *et al.*, 2012). This process leads to the formation of a thin layer of oxide on the metal alloy due to the high temperature of the two contacting surfaces, which leads to covering the wear surface and reducing the friction process over time, and weather

conditions play a decisive role in the rate of formation of this oxide (Venturi *et al*., 2020), The oxide layer can reform after fracturing under higher loads, especially if the temperature is high and the metal is exposed to air. The reformation rate of the oxide layer depends on factors such as temperature, load, and environmental conditions. Higher temperatures and specific weather conditions can accelerate the reformation of the oxide layer. The process of adhesion of the protrusions between the two sliding surfaces depends on the applied load and occurs in three stages. Initially, at low loads, a thin oxide layer forms, preventing actual contact between the two surfaces. As a result, the force required to break the bond between the protrusions is lower than the force between the alloy atoms, leading to low corrosion rates due to the absence of powdered oxide being ejected from the sample surface. This first stage, characterized by minimal wear, is referred to as light corrosion (Pulsford, 2022). As the load increases to intermediate levels, the oxide layer starts to break down, and the surfaces begin to make partial contact, causing a gradual increase in corrosion. At higher loads, the oxide layer is further disrupted, leading to more significant wear and the transition to severe corrosion. This stage is marked by higher wear rates and increased surface damage. Thus, the behavior changes gradually from light corrosion at low loads to severe corrosion at higher loads, with a noticeable intermediate stage of partial oxide breakdown and increasing surface contact.

The stage resulting from the increase in powdered oxide emitted from the sample is known as the transition corrosion stage, and can be observed at loading rates ranging from 14N to 18N (Rana *et al*., 2014). While the severe corrosion stage is considered the final stage, and occurs at loading rates exceeding 22N, where the alloy does not have enough time to form an oxide, resulting in the removal of thin layers from the surface of the alloy itself (Groover, 2007).

The stages mentioned above are an illustration of the sliding wear behavior of uncoated basic alloys. When comparing the wear rates between samples coated with different types of ceramic powders, it was found that these rates vary based on the nature and concentration of the coating powders used. Referring to the previous figure, we find that the coated sample (N_6) showed the lowest wear rate compared to the coated and uncoated alloys. The wear rate of these alloys decreased by-60.36% when applying a load of 26N, which represents more than half the wear rate of the uncoated alloys. This improvement in wear resistance is due to several factors, most notably that the coating gave the alloys higher hardness, which reduced the plastic deformation resulting from friction between the two surfaces (Dzhurinskiy *et al*., 2022). As observed when the load was increased to (26N), the formed oxide layer was destroyed, resulting in a strong metal contact protrusion, which makes the force required to cut or separate the connected protrusions higher than the strength of the alloy atoms, thus increasing the corrosion rates significantly. The reduced real contact area and lower shear force reduce the absence of sliding wear equations. The broken coating layer during wear acts as a lubricant due to the contact between the protrusions of the sliding surfaces, making the sliding weaker when the coating is present on one or both surfaces. This requires less shear force, which results in a reduced wear rate (Dzhurinskiy *et al*., 2022). In (Table 6), it is shown that the samples coated with various ceramic coatings showed a significant improvement in sliding wear resistance compared to the uncoated base alloy.

Table 6: Percentage improvement in sliding wear of coated alloys at load (26N).

No.	Sample code	Improvement percentage (%)	Load (N)
1	$N_\circ$	0	26
2	N_1	-8.95	26
3	N_2	-42.851	26
4	N_3	-42.466	26
5	N_4	-43.448	26
6	N_5	-58.554	26
7	N_6	-60.36	26
8	N_7	-46.28	26

After the coating process, all samples were heat treated at a temperature of $(900^{\circ}C)$, which increased the hardness of the alloy.

It is clear from Fig. (5) that the coated alloy (N_6), consisting of 75% silicon carbide (SiC) powder and 25% nickel-aluminum (Ni-Al) powder, showed the lowest rate of sliding wear compared to other samples. This indicates an improvement in the resistance to sliding wear depending on the type of coating used as well as the adhesion strength to resist the alloy from corrosion due to the adhesion strength between the silicon carbide particles on the one hand and the base alloy in addition to the nickel-aluminum bonding material on the other hand, while the other coated alloys had a clear effect on corrosion at varying rates.

Fig. (6) shows the relationship between the linear sliding velocity and the sliding wear rate, where it was observed that the wear rate for all coated and uncoated samples gradually decreases with increasing linear sliding velocity. When comparing the sliding wear behavior when changing the concentration of coating powders, it was observed that there is a clear decrease in the sliding wear rate for the coated alloy (N_6) consisting of (25 wt% Ni-Al) and (75 wt% SiC), which was the lowest compared to the rest of the coated and uncoated alloys. This is due to the rapid erosion of the coating layers, which led to filling the voids or cavities formed by the sliding process due to the high sliding velocity, forming a layer that isolates the alloy surface from the friction surface, which led to increased wear resistance and the adhesion of the separate coating particles as a result of the erosion process with the surface. Meanwhile, the coated alloy (N_1) consisting of the binder coating showed the highest

Sliding wear rates, and this comes as a result of the decrease in the bond strength between the coating layer and the base alloy, as a result of for the distortion process to occur. Because the heat generated by friction at low speeds is greater than at high speeds, this leads to increased softness of the protrusions at high speeds, which makes the force required to cut the contact points less than the bonding force of the alloy or coating metal atoms, and thus a decrease in the wear rate with an increase in the sliding speed.

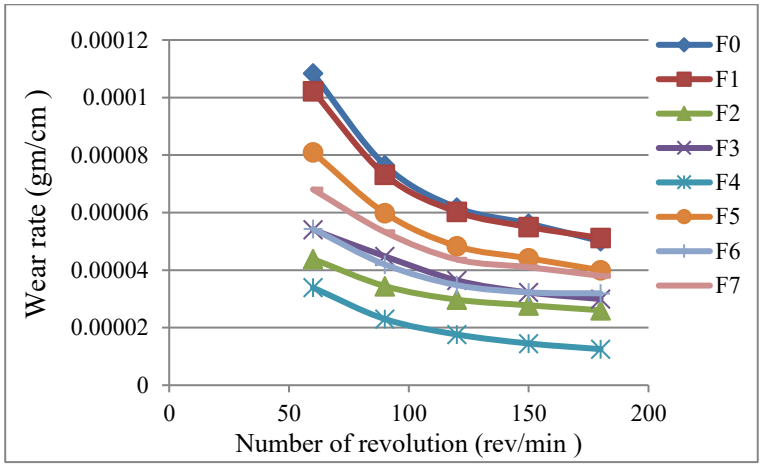

Fig. 6: Sliding wear rate of coated and uncoated samples at different speeds.

In (Table 7), we can see that the other coated samples showed significant improvement in sliding wear resistance compared to the uncoated base alloy. However, the coated sample N_1 showed a higher wear rate than all alloys except the uncoated base alloy, with an improvement of 2.25%.

Table 7: Increases in coated alloys' sliding wear rates at (180 rev/min).

No.	Sample code	Improvement percentage (%)	Number of revolution (rev/min)
1	N_1	2.25	180
2	N_2	-24.99	180
3	N_3	-18.35	180
4	N_4	-11.20	180
5	N_5	-16.14	180
6	N_6	-45.42	180
7	N_7	-43.42	180

When performing the sliding wear test by changing the nature of the abrasive surface, by changing the friction surfaces, shown in Fig. (8), it was found from the figure that the sliding wear rate decreases with increasing roughness of the granular surface. The reason for this is due to the small number of granules present on the surface area of the paper or the abrasive surface, i.e. in other words, the smoother the granular surface of the abrasive surface, the greater the amount of wear (Dzhurinskiy *et al*., 2022).

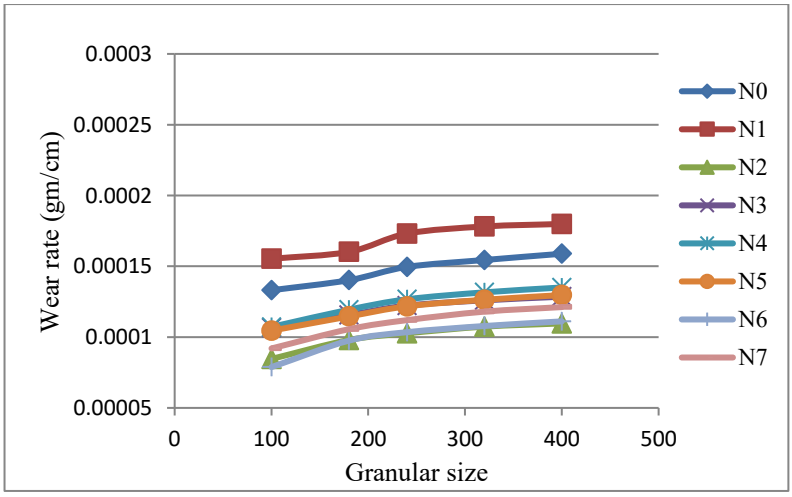

Fig. 8: Sliding wear rate of coated and uncoated samples at different grain surfaces.

As for the samples coated with the remaining ceramic coatings, we note that they also showed a significant improvement in varying percentages in the resistance to sliding wear, compared to the uncoated base alloy, shown in (Table 8), except for the coated sample (N_1), which demonstrated higher wear rates than the uncoated base alloy by (-13.24%).

Table 8: Percentage increase in coated alloys' sliding wear at a grain size of (400#) for the nature of the abrasive surface

No.	Sample code	Improvement Percentage (%)	Grain size of friction surface (#)
1	N_1	-13.24	400
2	N_2	-30.97	400
3	N_3	-19.09	400
4	N_4	-14.98	400
5	N_5	-18.37	400
6	N_6	-30.07	400
7	N_7	-23.71	400

CONCLUSIONS

The research evaluates how different ceramic powders including silicon oxide; silicon carbide combined with nickel-aluminum (SiC + SiO_2 + Ni-Al) influence the sliding corrosion behavior of AISI 446 stainless steel alloys. Studies evaluated the coatings' performance after steel samples got treated with thermal spraying methods through both sliding wear tests and corrosion testing methods. The applied coatings demonstrated substantial enhancement of the wear resistance in AISI 446 alloys beyond the uncoated base material properties. Under 26N vertical force the alloy containing 75% silicon carbide with 25% Ni-Al binder absorbed the most protection through a 60.36% decrease in corrosion while the wear rate showed increased rates in response to higher applied loads. The research discovered that the sliding wear rate directly depended on the number of ceramic particles in the covered layers. The alloy with 75% SiC and no SiO_2 exhibited the minimum wear rate at 180 rev/min which led to enhanced wear resistance performance. A subset of examined samples displayed wear rates exceeding those of both untreated alloy samples and particular experimental conditions. Thermal spray coatings show great potential according to study results for improving material resistance against sliding corrosion.

REFERENCES

Askeland, D.R.; Phulé, P.P.; Wright, W.J.; Bhattacharya, D.K. (2012). "The Science and Engineering of Materials". 6th ed., Cengage Learning, Inc.

Bandar, A.A.; Abbas, M.K.; Tuaimah, S.K. (2012). Study of the mechanical properties and wear resistance of aluminum-glass composites. *J. Eng. Tech.*, 2128.

Dzhurinskiy, D.; Babu, A.; Dautov, S.; Lama, A.; Mangrulkar, M. (2022). Modification of cold-sprayed Cu-Al-Ni-Al_2O_3 composite coatings by friction stir technique to enhance wear resistance performance. *Coat.*, **12**(8), 1113. DOI:10.3390/coatings12081113

Eyre, T.S. (1976). Wear characteristic of metal. *Trib. Inter.*, **9**(5), 203-212. DOI:10.1016/0301-679X(76)90077-3

Groover, M.P. (2007). "Fundamentals of Modern Manufacturing". 5th ed., John Wiley & Sons, New York.

Mazin, A.; Mahmood, A.; Gader, E.E. (2022). Effect of time on weight gain, thickness, cycle oxidation of thermal barrier coating (TBC) ZrO_2 at super alloy IN738LC. *Oxid. Comm.*, **45**(1), 186.

Pulsford, C. (2022). Microstructure characterisation of long-term aged advanced austenitic stainless steels for power plant applications. Loughborough University, Thesis. DOI: 10.26174/thesis.lboro. 21640946.v1

Rana, N.; Mahapatra, M.M.; Jayaganthan, R.; Prakash, S. (2014). Deposition of nanocrystalline coatings by modified LVOF thermal spray method. *J. Alloys Comp.*, **615**, 779-783. DOI: 10.1016/j.jallcom.2014.07.038

Tao, K.; Zhou, X.; Cui, H.; Zhang, J. (2009). Microhardness variation in heat-treated conventional and nanostructured NiCrC coatings prepared by HVAF spraying. *Sur. Coat. Tech.*, **203**, 1406–1414. DOI: 10.1016/j.surfcoat.2008.11.020

Tsukizoe, T.; Ohmae, N. (1983). Friction and wear of advanced composite materials. *Fib. Sci. Tech.*, **18**(4), 265-286. DOI:10.1016/0015-0568(83)90021-0

Vafaeenezhad, H.; Zebarjad, S.M.; Khaki, J.V. (2012). Fabrication and wear behavior investigation of the carbon/epoxy composites based on wood using artificial neural networks. *Adv. Mater. Res.*, **413**, 95-102. DOI: 10.4028/www.scientific.net/AMR.413.95

Venturi, F.; Pulsford, J.; Hussain, T. (2020). A novel approach to incorporating graphene nanoplatelets into Cr_2O_3 for low-wear coatings. *Mater. Lett.*, **276**, 128-283. DOI: 10.1016/j.matlet.2020.128283

Wang, B.Q.; Lee, S.W. (1997). Elevated temperature erosion of several thermal-sprayed coatings under the simulated erosion conditions of in-bed tubes in a fluidized bed combustor. *Wear*, **203**, 580-587. DOI:10.1016/S0043-1648(96)07381-4

دراسة تأثير استخدام مساحيق سيراميكية مختلفة في تقنية الرش الحراري على مقاومة التآكل الانزلاقي لسبائك الصلب (AISI446)

أحمد صبحي علي حسين يحيى عبد الكريم سلمان إدريس عيدان غدير

قسم الفيزياء/ كلية العلوم/ جامعة الموصل/ الموصل/ العراق

الملخص

تتطلب الظواهر المختلفة قياسًا منفصلًا لمعدل التآكل ومعدل التآكل الناتج عن الانزلاق. يحدث التآكل نتيجة للتحلل الكيميائي بين المواد المتلامسة وبيئاتها، بينما يسبب الاحتكاك الناتج عن الأسطح المتحركة التآكل الناتج عن الانزلاق. درس العلماء مقاومة التآكل الناتج عن الانزلاق لسبيكة الفولاذ المقاوم للصدأ AISI 446 التي تلقت طبقات حرارية مصنوعة من تركيزات مختلفة من أكسيد السيليكون وكربيد السيليكون ونيكل–ألومنيوم ($SiC + SiO_2 + Ni\text{-}Al$) معاجين السيراميك. تم استخدام شعلة لحام حراري (QH-2/H) كأداة لتطبيق الطلاءات. تم اتباع إجراءات الاختبار وفقًا للمواصفات القياسية ASTM D5963 باستخدام جهاز المحور على القرص الذي يعمل مع أحمال رأسية مختلفة بسرعات ومعلمات سطح القرص. كشفت التحليلات التجريبية أن الطلاءات المستخدمة أظهرت مقاومة أعلى للتآكل الناتج عن الانزلاق مقارنةً بالمزيج الأساسي بعد تضمينها. ارتفع معدل التآكل لجميع العينات المختبرة بشكل تدريجي مع زيادة الأحمال. حققت السبيكة N_1 أدنى معدل تآكل حيث تحتوي على 75% من كربيد السيليكون مدموجًا مع 25% من مادة الرابط Ni-Al. أظهرت السبيكة انخفاضًا قدره −60.36% في معدل التآكل مقارنة بالسبيكة الأصلية عند تعرضها لقوة رأسية قدرها N26. بينما السبيكة N_6 المكونة من 75% SiC ومن دون SiO_2 أظهرت أقل معدل تآكل انزلاقي قدره 180 دورة/دقيقة بسبب أدائها المحسن بنسبة −45.42%. أما العينة N_1 فقد أظهرت أداءً أقل مقارنة بالسبيكة غير المطلية على الرغم من أن سطحها الكاشط أحدث مقاومة أفضل للتآكل. أظهرت النتائج زيادة في معدل التآكل بنسبة −13.24%.

الكلمات الدالة: السبائك، مقاومة التآكل الانزلاقي، الرش الحراري.